

# Search for GeV and X-ray flares associated with the IceCube track-like neutrinos

Fang-Kun Peng<sup>1,2</sup>, Xiang-Yu Wang<sup>1,2</sup>

## ABSTRACT

Dozens of high-energy neutrinos have been detected by the IceCube neutrino telescope, but no clear association with any classes of astrophysical sources has been identified so far. Recently, Kadler et al. (2016) report that a PeV cascade-like neutrino event occurs in positional and temporal coincidence with a giant gamma-ray flare of the blazar PKS B1424-418. Since IceCube track-like events have much better angular resolution, we here search for possible short-term gamma-ray flares that are associated with the IceCube track-like events with *Fermi* Large Area Telescope (LAT) observations. Among them, three track-like neutrino events occur within the field of view of *Fermi*-LAT at the time of the detection, so search for the *prompt* gamma-ray emission associated with neutrinos are possible. Assuming a point source origin and a single power law spectrum for the possible gamma-ray sources associated with neutrinos, a likelihood analysis of 0.2-100 GeV photons observed by *Fermi*-LAT on the timescales of  $\sim 12$  hours and one year are performed, and for the three special neutrinos, the analysis are also performed on the timescales of thousand of seconds before and after the neutrino detection. No significant GeV excesses over the background are found and the upper limit fluxes at 95% confidence level are obtained for different timescales. We also search for possible hard X-ray transient sources associated with the IceCube track-like neutrino events, but the search also yields null results. We discuss the implication of the non-detection of gamma-ray flares for the constraints on the neutrino source density.

*Subject headings:* neutrinos–galaxies: active–gamma rays

---

<sup>1</sup>School of Astronomy and Space Science, Nanjing University, Nanjing 210093, China; xywang@nju.edu.cn

<sup>2</sup>Key laboratory of Modern Astronomy and Astrophysics (Nanjing University), Ministry of Education, Nanjing 210093, China

## 1. Introduction

The IceCube telescope has detected TeV-PeV neutrinos from extraterrestrial sources for the first time (IceCube Collaboration 2013; Aartsen et al. 2014; The IceCube Collaboration et al. 2015), which open a new window to explore the high-energy universe. The explanation of a single atmospheric origin of these high-energy neutrino events collected during 4 years has been strongly disfavored at around  $6.5\sigma$  level of confidence (Aartsen et al. 2014; The IceCube Collaboration et al. 2015). The best fit result for the high-energy astrophysical neutrino flux reaches a level of  $E_\nu^2 \Phi_\nu \sim 10^{-8} \text{ GeV cm}^{-2} \text{ s}^{-1} \text{ sr}^{-1}$  per flavor between around 60 TeV and 2 PeV, and the spectral index of the power law model is  $-2.5 \sim -2.0$  (Aartsen et al. 2014, 2015a).

The astrophysical neutrinos have shown no significantly directional clustering (Aartsen et al. 2014). They also show no clear association with any known classes of astrophysical sources so far. High-energy neutrino emission results from the decays of charged pions produced in the interaction between relativistic protons and ambient gas ( $pp$ ) or ambient radiation ( $p\gamma$ ), and the same processes inevitably produce high-energy gamma-ray photons via the neutral pion decays. Although very high-energy photons above, e.g. 100 GeV, may be absorbed in the source or during the propagation in the intergalactic space, GeV photons could escape and arrive at the Earth accompanying neutrinos. The potential astrophysical sources to produce high-energy neutrinos and photons include star-forming galaxies (Loeb & Waxman 2006; He et al. 2013; Murase et al. 2013; Anchordoqui et al. 2014; Liu et al. 2014; Tamborra et al. 2014; Wang et al. 2014; Chang et al. 2015), tidal disruption events (Wang & Liu 2016), gamma-ray bursts (GRBs) (Waxman & Bahcall 1997; Cholis & Hooper 2013; Liu & Wang 2013; Murase & Ioka 2013), active galactic nucleus (AGNs) (Anchordoqui et al. 2008; Kalashev et al. 2013; Stecker 2013; Murase et al. 2014; Dermer et al. 2014), double white dwarf mergers (Xiao et al. 2016) and even Galactic sources (Fox et al. 2013; Razzaque 2013; Ahlers & Murase 2014; Lunardini et al. 2014; Neronov et al. 2014), see Ahlers & Halzen (2015) for a review. However, combined data analysis between IceCube neutrinos events and  $\gamma$ -ray sources sample, such as GRBs, AGNs, soft  $\gamma$ -ray repeaters, supernova remnants, pulsars, microquasars, and X-ray binaries (Padovani & Resconi 2014; Krauß et al. 2014; Aartsen et al. 2015a,b; Padovani et al. 2016; Glüsenkamp 2016; Aartsen et al. 2016; Wang & Li 2016), do not reveal any firm associations up to now.

Recently Kadler et al. (2016) find that a cascade-like PeV neutrino event occurs in positional and temporal coincidence with a giant gamma-ray flare of the flat spectrum radio quasars (FSRQs) PKS B1424-418, with a chance probability of 5% for such coincidence (i.e., a  $2\sigma$  confidence level correlation). This cascade-like neutrino has an angular error of  $\sim 15^\circ$ . In contrast to cascade-like events, the median angular resolution of muon track

neutrino events are much better ( $\simeq 1^\circ$ ), and hence they are good candidates to search for the electromagnetic counterparts. Brown et al. (2015) have performed the search for the gamma-ray counterparts of the first 7 IceCube track-like neutrinos ( $E_\nu > 30$  TeV) using 70-month *Fermi*-LAT data, and no steady  $\gamma$ -ray counterparts are found. For the purpose of examining whether short-term transient sources like PKS B1424-418 are associated with neutrinos, we here search for possible transient gamma-ray counterparts (on the timescale as short as hours) of 12 track-like events<sup>1</sup> observed by IceCube up to August 6, 2016 (Aartsen et al. 2014; The IceCube Collaboration et al. 2015; Schoenen & Raedel 2015; Blaufuss 2016). We select neutrino events with energies larger than 60 TeV to reduce the contamination from the atmospheric background (Aartsen et al. 2014). This analysis method is rather than cross-correlating with known catalogs, but uses the *Fermi*-LAT survey data to search for new  $\gamma$ -ray transients related with the IceCube track-like events or flux variability of known  $\gamma$ -ray sources. Different from Brown et al. (2015), our work aims to find possible short-term or prompt GeV emission associated with these neutrinos, such as X-ray transients or gamma-ray transients (e.g. AGN gamma-ray flares), which could be missed in the 70-month long timescale analysis similar to Brown et al. (2015). We note that the gamma-ray flare of PKS B1424-418 is extremely strong and lasts for more than one year. Sources with flares at such flux level and durations from neutrino directions examined in Brown et al. (2015) would have been observed as a significant excesses. However, for sources like short-term bright flare of AGNs or GRBs, the signal may be diluted and become undetectable in a longer time interval. Our analysis is most sensitive to gamma-ray sources that are transient only in a short time interval and are quiescent over a long time interval. For example, a radio-intermediate quasars III Zw 2 exhibits distinct GeV flares in the short term, but no significant gamma-ray signal has been detected in the time-averaged 7-year *Fermi*-LAT data (Liao et al. 2016). *Fermi* All-sky Variability Analysis has found that, among 518 flaring gamma-ray sources, 77 sources lack of gamma-ray counterparts in the 7.4 years of *Fermi* observations (Abdollahi et al. 2016). Some tidal disruption events (TDEs) show short-duration luminous X-ray flares. Although high-energy emissions from TDEs have not been detected by *Fermi*-LAT so far (Peng et al. 2016), they are potential sources of giant gamma-ray flares (Farrar & Gruzinov 2009). GRBs also have bright GeV emission during the prompt and afterglow phase, although there is no evidence of association with IceCube high-energy neutrinos so far. Our analysis would be sensitive to such short-term gamma-ray transients.

The organization of the paper is as follows. In section 2, we describe the search results with the *Fermi*-LAT observations, the result for the search of the *Swift* hard X-ray transient

---

<sup>1</sup>[http://gc.n.gsfsc.nasa.gov/amon\\_hese\\_events.html](http://gc.n.gsfsc.nasa.gov/amon_hese_events.html), [http://gc.n.gsfsc.nasa.gov/amon\\_ehe\\_events.html](http://gc.n.gsfsc.nasa.gov/amon_ehe_events.html)

sources is described in section 3. In section 4, we discuss the implication of the non-detection of gamma-ray transients for constraining the source number density. Finally we give the conclusions and discussions in section 5.

## 2. *Fermi* data reduction

### 2.1. *Fermi*-LAT data analysis

The newly released *Fermi*-LAT (Atwood et al. 2009) Pass 8 SOURCE data (P8R2 Version 6) and *Fermi* science tools version v10r0p5 are used in the present work. An unbinned maximum likelihood analysis is performed on a region of interest (ROI) with a radius  $10^\circ$  centered on the right ascension and declination of the each IceCube track-like neutrino. All FRONT+BACK converting photons with energies between 0.2-100 GeV are taken into consideration. We apply the maximum zenith-angle cut  $z_{max} = 90^\circ$  to eliminate the Earth’s limb emission. The expression of  $(\text{DATA\_QUAL} > 0) \ \& \ (\text{LAT\_CONFIG} == 1)$  is used to further filter the data. A source model is generated containing the position and spectral definition for all the point sources and diffuse emission from the 3FGL (Acero et al. 2015) within  $15^\circ$  of the ROI center. The Galactic and extragalactic diffuse models are `gll_iem_v06.fits` and `iso_P8R2_SOURCE_V6_v06.txt`, respectively. We add a point source with power-law spectrum ( $dN/dE = A \times (E/E_0)^{-\Gamma}$ ) on each track-like neutrino position in the source model file. Since we pay attention to the short-term behavior of  $\gamma$ -ray emission on the timescales of hours or months, the spectral indices of all point sources in the source model file are fixed to their 3FGL catalogue values to solve convergence problems. The normalization factors of point sources, the extragalactic diffuse emission, and the Galactic diffuse emission are left free to vary. After each successful fit, test-statistic (TS) map centered on the neutrino position is created to check if there is any excess  $\gamma$ -ray emission above the background beyond the 3FGL catalog. All the upper limit fluxes are reported at the 95% confidence level with fixed spectral index  $\Gamma = 2$ . We have tested that assuming different spectral indices would result in a slight but insignificant difference.

### 2.2. *Fermi*-LAT data search results

We first perform the data analysis over  $\sim 12$  hours, i.e. 6 hours before and 6 hours after the neutrino detection time, to search for possibly prompt GeV emission accompanying these neutrino events. No significant gamma-ray emissions at the position of the track-like neutrino events are found, and thus their upper limit fluxes are obtained, see Table 1 and

Figure 1. There is no new  $\gamma$ -ray source around the region of the neutrino position identified by checking the TS map. For comparison, the *Fermi*-LAT data analysis for the gamma-ray flaring blazar PKS B1424-418 in a similar time period (centering at the detection time of the neutrino event number 35 ) is also carried out and the result is presented in Table 1 and Figure 1. For the same period of time, PKS B1424-418 shows bright emission with detection significance of  $TS = 57$ , and the photon flux is  $3.54 \pm 0.99 \times 10^{-7}$  ph cm $^{-2}$  s $^{-1}$  (i.e. the corresponding energy flux is  $4.05 \pm 1.14 \times 10^{-10}$  erg cm $^{-2}$  s $^{-1}$  in 0.2 – 100 GeV). As we can see in Figure 1, the upper limit fluxes of any possible point sources associated with the track-like neutrinos are below the flux of the PKS B1424-418. We also find that all the 3FGL sources within the  $2R_{50}$  angular error of track-like neutrinos are too weak to be detected by *Fermi*-LAT for twelve-hour observations (here  $R_{50}$  means angular error at the 50% confidence level).

As some blazars outbursts occur on the timescale of months, we further choose one year for the time window to search for gamma-ray flares. The likelihood analysis of *Fermi*-LAT data of each track-like neutrino event is conducted, which also yields a null result. The upper limit fluxes covering the period of half year before and half year after the neutrino detection time are given in Table 1 and also shown in Figure 2. Similarly, over one year *Fermi*-LAT observation centering at the detection time of the neutrino event number 35, PKS B1424-418 shows high photon flux  $5.89 \pm 0.06 \times 10^{-7}$  ph cm $^{-2}$  s $^{-1}$  ( $TS = 50770$ ), which corresponds to an energy flux of  $8.17 \pm 0.14 \times 10^{-10}$  erg cm $^{-2}$  s $^{-1}$ . The upper limit gamma-ray fluxes for the track-like neutrinos are far below the flux of PKS B1424-418. We note that neutrino event number 5 has a known 3FGL  $\gamma$ -ray source J0725.8-0054 (BL Lac object PKS 0723-008) located  $\sim 1^\circ$  from neutrino’s position. Another 3FGL  $\gamma$ -ray source J2227.8+0040 (BL Lac object PMN J2227+0037) is located  $\sim 0.7^\circ$  from the number 44 neutrino event. The two sources are detected at  $TS = 83$  and  $TS = 35$  in one year observation respectively. The one year fluxes of the two sources are consistent with the values published in the 3FGL catalogue, which are two orders of magnitude lower than that of PKS B1424-418. While these two 3FGL sources appear to have a hard spectral index, there is no evidence that they are TeV gamma-ray sources (<http://tevcat.uchicago.edu/>). Moreover, when a spatial error of  $2R_{50}$  is considered, additional 9 3FGL sources, most of which are blazars, are in positional agreement with the these track-like neutrino events (see Table 2 for more details). Their gamma-ray fluxes are, however, too low to account for the observed neutrino flux, in contrast to PKS B1424-418. No new  $\gamma$ -ray source around the region of the neutrino position is discovered.

We calculate the significance of the spatial coincidence of 3FGL sources with the IceCube track-like neutrinos, running 10000 simulations in which the declination and the right ascension of each 3FGL sample are randomized. For each simulation, we obtain a count

number  $n$  of 3FGL sources within  $R_{50}$  of our track-like neutrino events sample. The chance probability is calculated as the ratio between the number of the simulations that have  $n \geq 2$  and the total number of simulations. This approach results in a chance probability  $\sim 98\%$ , suggests that the coincidence between two 3FGL sources, J0725.8-0054 (PKS 0723-008) and J2227.8+0040 (PMN J2227+0037), and the track-like neutrino events is merely by chance. If the declination is fixed and the right ascension is randomized only, the chance probability of such spatial coincidence reaches  $\sim 83\%$ . We therefore find no evidence of gamma-ray emission associated with the IceCube track-like neutrino events. Considering the  $\gamma$ -ray flux limits for one year *Fermi*-LAT observation, we suggest that any gamma-ray flares that are associated with the IceCube track-like neutrino events must be at least one order of magnitude dimmer than that of PKS B1424-418<sup>2</sup> (see Figure 2).

### 2.3. IceCube neutrino events number 23, 45 and 160806A

We note that three IceCube track-like neutrino events, e.g. number 23, 45 and 160806A, locate at small angle ( $< 70^\circ$ ) from *Fermi*-LAT boresight at the neutrino detection time. In other words, the region around the track-like neutrino events is within the *Fermi*-LAT field of view during the  $\sim 1000$ s before and after the neutrino detection. Therefore the above three neutrinos are very suitable for searching for the prompt GeV emission accompanying the neutrino emission. The angular distance between neutrino position and *Fermi*-LAT boresight (denoted as  $\Theta$ ) versus time is shown in Figure 3. The time intervals for *Fermi*-LAT data analysis are selected with the criterion  $\Theta < 70^\circ$ , which are also presented in Table 3. The likelihood analysis centered on each neutrino position result in upper limit fluxes given in Table 3. No new  $\gamma$ -ray point sources are found within  $2R_{50}$  of the neutrinos position. For the neutrino event number 23, there are four 3FGL sources within  $2R_{50}$ , while for the other two neutrino events, there are no sources within  $2R_{50}$ . The four 3FGL sources mentioned above are very weak, and none of them shows any significant detection over  $\sim 1000$  s of *Fermi*-LAT observations. In brief, we find no evidence of prompt GeV emissions following the IceCube track-like neutrino events.

---

<sup>2</sup>Interestingly, Gao et al. (2016) find that a hybrid model with sub-dominant hadronic component is needed to explain the multi-waveband observation of PKS B1424-418 flare.

### 3. Cross-correlation with *Swift* hard X-ray transient sources

The high-energy photons from pion decay could be accompanied by X-ray emissions that are produced by secondary electrons and positrons via, e.g. synchrotron radiation in the magnetic fields of the source (Kistler 2015; Murase et al. 2016). *Swift* Burst Alert Telescope (BAT) is very useful for discovering new X-ray transient sources or detecting the flux variability of known X-ray sources (Barthelmy et al. 2005; Krimm et al. 2013). We thus make a cross-correlation analysis between *Swift*/BAT transient sources catalog and the IceCube track-like neutrino events. The catalog includes 1009 X-ray transient sources (see <http://swift.gsfc.nasa.gov/results/transients/>), including Galactic and extragalactic sources. None *Swift*/BAT transient source is found inside the error box  $R_{50}$  of the IceCube track-like neutrino events. Within  $2R_{50}$ , four *Swift*/BAT transient sources are in positional agreement with the IceCube track-like neutrino events number 23, 44 and 47 (see Table 4). To investigate their temporal characteristics around the time that the corresponding neutrino events are detected, we extract the day-bin light curves for these X-ray sources. No significant flares are observed at the neutrino detection time for the four X-ray transient sources, as shown in Figure 4. Similarly, a chance probability of  $\sim 60\%$  for the positional coincidence is estimated using Monte Carlo simulations with the sample data randomized in right ascension. Therefore, considering the insignificant spatial coincidence and the observed temporal behavior of the X-ray transients, we suggest that these *Swift*/BAT transient sources are not in physical association with the IceCube track-like neutrino events.

### 4. Implications for constraining the neutrino source density

The production of neutrinos are accompanied by high-energy gamma-rays, so the point source gamma-ray flux limits could, in principle, provide useful constraints on the neutrino sources. For  $pp$  collision mechanism of TeV-PeV neutrinos, one expect that GeV gamma-ray flux lies at the power-law extrapolation of TeV gamma-rays. The gamma-ray flux scales with the neutrino flux through the relation  $F_\gamma \simeq 2(E_\gamma/2E_\nu)^{2-p}F_\nu$  (Murase et al. 2013), assuming that the parent cosmic rays are produced with a power-law spectrum,  $dN_{CR}/dE_{CR} \propto E_{CR}^{-p}$ . For  $p\gamma$  mechanism, the flux of hadronic GeV gamma-rays depends on the properties of soft target photons in the source. For simplicity, below we assume that  $F_\nu(60 - 2000\text{TeV}) = \eta F_\gamma(0.2 - 100\text{GeV})$ , with  $\eta \simeq 0.5$  for  $p = 2$  in the  $pp$  interaction model. We assume that the sources are transparent to gamma-rays, i.e. they are not the hidden sources in gamma-rays. Our study has found that the sources of the track-like neutrino events should be weak in  $\gamma$ -rays in 0.2-100 GeV, even during the neutrino emitting period. Given a measured neutrino background flux by IceCube, one can obtain a lower limit on the source number density with

the upper limit on the neutrino luminosity of individual sources under the above assumptions. The observed background neutrino flux implies a local energy production rate of

$$n_0 L_\nu \simeq 3 \times 10^{44} \text{ erg Mpc}^{-3} \text{ yr}^{-1} \left( \frac{\xi_z}{3} \right)^{-1} \left( \frac{\sum_i E_{\nu,i}^2 \Phi_{\nu,i}}{3 \times 10^{-8} \text{ GeV cm}^{-2} \text{ s}^{-1} \text{ sr}^{-1}} \right), \quad (1)$$

where  $n_0$  is the local number density,  $L_\nu$  is the averaged neutrino luminosity of the each source throughout the universe,  $\xi_z$  is a dimensionless parameter that accounts for the redshift evolution of the sources, and  $\sum_i E_{\nu,i}^2 \Phi_{\nu,i}$  is the all-flavor neutrino flux. The upper limit gamma-ray flux for one year *Fermi*-LAT observations is on average  $F_\gamma \lesssim 7 \times 10^{-13} \text{ erg cm}^{-2} \text{ s}^{-1}$ , so the limit on the neutrino flux of an individual source is also  $F_\nu \lesssim 7 \times 10^{-13} \eta \text{ erg cm}^{-2} \text{ s}^{-1}$ . As the neutrino source density is expected to peak at  $z \sim 1 - 2$  following the cosmic star formation rate, we take the luminosity distance of these neutrino sources as  $d_L = 10^{28} \text{ cm}$  (Chang et al. 2016)<sup>3</sup>. Then we obtain an upper limit of the neutrino luminosity of an individual source

$$L_\nu \lesssim 4\pi d_L^2 F_\nu \simeq 9 \times 10^{44} \eta \text{ erg s}^{-1}. \quad (2)$$

Thus, a lower limit on the continuous source density under the above assumptions may be written as

$$n_0 \gtrsim 10^{-8} \text{ Mpc}^{-3} \eta^{-1} \left( \frac{\xi_z}{3} \right)^{-1} \left( \frac{F_\gamma}{7 \times 10^{-13} \text{ erg cm}^{-2} \text{ s}^{-1}} \right)^{-1}. \quad (3)$$

For short-term transient neutrino sources, the upper limit gamma-ray flux for  $\sim 1000 \text{ s}$  observations is about  $F_\gamma \approx 5 \times 10^{-10} \text{ erg cm}^{-2} \text{ s}^{-1}$ , so the energy released in neutrinos per event should be smaller than  $7 \times 10^{50} \eta \text{ erg}$ . Using a similar approach, we find a lower limit on the event rate of the transients, i.e.,

$$\dot{n}_0 \gtrsim 4 \times 10^2 \text{ Gpc}^{-3} \text{ yr}^{-1} \eta^{-1} \left( \frac{\xi_z}{3} \right)^{-1} \left( \frac{F_\gamma}{5 \times 10^{-10} \text{ erg cm}^{-2} \text{ s}^{-1}} \right)^{-1}. \quad (4)$$

We would like to stress that the above lower limits are obtained based on the assumptions mentioned at the beginning of this section. The validity of these assumptions depends heavily on the relation between photon and neutrino fluxes. The limits are useful for constraining the source models. FSRQs have a number density of  $\sim 10^{-9} \text{ Mpc}^{-3}$  and a faster redshift evolution than the cosmic star formation rate (Ajello et al. 2012, 2014). Taking  $\xi_z \simeq 8.4$  for FSRQs, they are only marginally consistent with the above constraint. Starburst galaxies,

---

<sup>3</sup>Though different objects show different evolution scenarios, hence different  $\xi_z$ , FSRQs and star-forming galaxies both have a space density peaking at modest redshift  $z \approx 1$ . Thus the luminosity distance of  $d_L = 10^{28} \text{ cm}$  is a plausible assumption in the ensuing discussion.



one the other hand, have a number density of  $\sim 10^{-4} \text{ Mpc}^{-3}$  (Ackermann et al. 2012), so they fully satisfy the above constraints for a large parameter space of  $\eta$ . For short-term transient sources, since high-luminosity GRBs have a density of  $\sim 1 \text{ Gpc}^{-3} \text{ yr}^{-1}$ , one can rule out GRBs as the main contributing sources of these neutrinos if  $\eta < 100$  (i.e. the neutrino flux at TeV-PeV energies is a factor of  $< 100$  larger than that in GeV gamma-rays). Since low-luminosity GRBs have a density of  $200 - 1000 \text{ Gpc}^{-3} \text{ yr}^{-1}$ , they can not be ruled out by our *Fermi*-LAT data analysis. We note that the constraints on the source density are generally consistent with the results obtained by using the non-detection of high-energy neutrino multiplets in the IceCube data (Ahlers & Halzen 2014; Murase & Waxman 2016).

## 5. Conclusions and Discussions

By using *Fermi*-LAT observations, we searched for  $\gamma$ -ray transient emission on the timescales of hours to months coincident with the IceCube track-like neutrino events above 60 TeV. The null result suggests that any associated gamma-ray flares must be at least one order of magnitude dimmer than that of the blazar PKS B1424-418, for which a PeV cascade-like neutrinos is claimed to be associated at 95% confidence level. For three track-like neutrinos that occurred within the field of view of *Fermi*-LAT at the time of the neutrino detection, we also searched for prompt GeV emission coincident in time with these neutrinos. No significant GeV emissions associated with these neutrino events are found. A few 3FGL  $\gamma$ -ray objects locate within  $2R_{50}$  of the neutrino position, but the probability for chance coincidence is large. They are also too weak in gamma-ray emission to be reconciled with the neutrino emission. Based on the non-detections of GeV emissions and some assumptions (see Section 4), the inferred local number density for continuous emitting sources to produce high-energy neutrinos should be  $n_0 \gtrsim 10^{-8} \text{ Mpc}^{-3}$  by assuming a flat gamma-ray spectrum resulted from the  $pp$  mechanism for neutrinos. Similarly, for transient sources, we obtain an event rate of  $\dot{n}_0 \gtrsim 4 \times 10^2 \text{ Gpc}^{-3} \text{ yr}^{-1}$ . We also searched for possible hard X-ray transients observed by *Swift*/BAT that are coincident with the track-like neutrino events, but no X-ray flares are found to be spatially and temporally coincident with these neutrino events.

Some alternative explanations for non-detection of 0.2-100 GeV emission accompanying the IceCube track-like neutrino events are possible. For example, if the high-energy photons produced in the pion mesons process can not escape freely from the source region (i.e. the hidden sources in gamma-rays), they would not suffer from the above constraints. Another possibility is that the gamma-ray luminosity at GeV energies is far below that of the TeV-PeV neutrinos in the  $p\gamma$  scenario when the energy threshold of cosmic rays for pion production in interactions with radiation fields is too high. Future prompt follow-up observations in TeV

energies by Imaging Cherenkov Telescopes, such as CTA, HAWC and LHAASO, would be useful to test the latter possibility.

### Acknowledgments

We thank Ruo-Yu Liu and Xiao-Chuan Chang for useful discussions. We also acknowledge a constructive report from the referee. This work has made use of data and software provided by the *Fermi* Science Support Center, and *Swift*/BAT transient monitor results provided by the *Swift*/BAT team. This work is supported by the 973 program under grant 2014CB845800, the NSFC under grants 11625312 and 11273016.

### REFERENCES

- Aartsen, M. G., Abraham, K., Ackermann, M., et al. 2016, *ApJ*, 824, 115
- Aartsen, M. G., Abraham, K., Ackermann, M., et al. 2015a, *ApJ*, 809, 98
- Aartsen, M. G., Ackermann, M., Adams, J., et al. 2015b, *ApJ*, 807, 46
- Aartsen, M. G., Ackermann, M., Adams, J., et al. 2014, *Physical Review Letters*, 113, 101101
- Abdollahi, S., Ackermann, M., Ajello, M., et al. 2016, arXiv:1612.03165
- Acerro, F., Ackermann, M., Ajello, M., et al. 2015, *ApJS*, 218, 23
- Ackermann, M., Ajello, M., Allafort, A., et al. 2012, *ApJ*, 755, 164
- Ahlers, M., & Halzen, F. 2015, *Reports on Progress in Physics*, 78, 126901
- Ahlers, M., & Halzen, F. 2014, *Phys. Rev. D*, 90, 043005
- Ahlers, M., & Murase, K. 2014, *Phys. Rev. D*, 90, 023010
- Ajello, M., Romani, R. W., Gasparrini, D., et al. 2014, *ApJ*, 780, 73
- Ajello, M., Shaw, M. S., Romani, R. W., et al. 2012, *ApJ*, 751, 108
- Anchordoqui, L. A., Hooper, D., Sarkar, S., & Taylor, A. M. 2008, *Astroparticle Physics*, 29, 1
- Anchordoqui, L. A., Paul, T. C., da Silva, L. H. M., Torres, D. F., & Vlcek, B. J. 2014, *Phys. Rev. D*, 89, 127304

- Atwood, W. B., Abdo, A. A., Ackermann, M., et al. 2009, *ApJ*, 697, 1071
- Barthelmy, S. D., Barbier, L. M., Cummings, J. R., et al. 2005, *Space Sci. Rev.*, 120, 143
- Blaufuss, E. 2016, *GRB Coordinates Network*, 19363, 1
- Brown, A. M., Adams, J., & Chadwick, P. M. 2015, *MNRAS*, 451, 323
- Chang, X.-C., Liu, R.-Y., & Wang, X.-Y. 2016, *ApJ*, 825, 148
- Chang, X.-C., Liu, R.-Y., & Wang, X.-Y. 2015, *ApJ*, 805, 95
- Cholis, I., & Hooper, D. 2013, *J. Cosmology Astropart. Phys.*, 6, 030
- Cowen, D. F. 2016, *GRB Coordinates Network*, 19787, 1
- Dermer, C. D., Murase, K., & Inoue, Y. 2014, *Journal of High Energy Astrophysics*, 3, 29
- Farrar, G. R., & Gruzinov, A. 2009, *ApJ*, 693, 329
- Fox, D. B., Kashiyama, K., & Mészáros, P. 2013, *ApJ*, 774, 74
- Gao, S., Pohl, M., & Winter, W. 2016, *arXiv:1610.05306*
- Glüsenkamp, T. 2016, *European Physical Journal Web of Conferences*, 121, 05006
- He, H.-N., Wang, T., Fan, Y.-Z., Liu, S.-M., & Wei, D.-M. 2013, *Phys. Rev. D*, 87, 063011
- IceCube Collaboration 2013, *Science*, 342, 1242856
- Kadler, M., Krauß, F., Mannheim, K., et al. 2016, *arXiv:1602.02012*
- Kalashev, O. E., Kusenko, A., & Essey, W. 2013, *Physical Review Letters*, 111, 041103
- Kistler, M. D. 2015, *arXiv:1511.01530*
- Krauß, F., Kadler, M., Mannheim, K., et al. 2014, *A&A*, 566, L7
- Krimm, H. A., Holland, S. T., Corbet, R. H. D., et al. 2013, *ApJS*, 209, 14
- Liao, N.-H., Xin, Y.-L., Fan, X.-L., et al. 2016, *ApJS*, 226, 17
- Liu, R.-Y., & Wang, X.-Y. 2013, *ApJ*, 766, 73
- Liu, R.-Y., Wang, X.-Y., Inoue, S., Crocker, R., & Aharonian, F. 2014, *Phys. Rev. D*, 89, 083004

- Loeb, A., & Waxman, E. 2006, *J. Cosmology Astropart. Phys.*, 5, 003
- Lunardini, C., Razzaque, S., Theodoseou, K. T., & Yang, L. 2014, *Phys. Rev. D*, 90, 023016
- Murase, K., Ahlers, M., & Lacki, B. C. 2013, *Phys. Rev. D*, 88, 121301
- Murase, K., Guetta, D., & Ahlers, M. 2016, *Physical Review Letters*, 116, 071101
- Murase, K., Inoue, Y., & Dermer, C. D. 2014, *Phys. Rev. D*, 90, 023007
- Murase, K., & Ioka, K. 2013, *Physical Review Letters*, 111, 121102
- Murase, K., & Waxman, E. 2016, arXiv:1607.01601
- Neronov, A., Semikoz, D., & Tchernin, C. 2014, *Phys. Rev. D*, 89, 103002
- Padovani, P., & Resconi, E. 2014, *MNRAS*, 443, 474
- Padovani, P., Resconi, E., Giommi, P., Arsioli, B., & Chang, Y. L. 2016, *MNRAS*, 457, 3582
- Peng, F.-K., Tang, Q.-W., & Wang, X.-Y. 2016, *ApJ*, 825, 47
- Razzaque, S. 2013, *Phys. Rev. D*, 88, 081302
- Schoenen, S., & Raedel, L. 2015, *The Astronomer’s Telegram*, 7856,
- Stecker, F. W. 2013, *Phys. Rev. D*, 88, 047301
- Tamborra, I., Ando, S., & Murase, K. 2014, *J. Cosmology Astropart. Phys.*, 9, 043
- The IceCube Collaboration, Aartsen, M. G., Abraham, K., et al. 2015, arXiv:1510.05223
- Wang, B., & Li, Z. 2016, *Science China Physics, Mechanics, and Astronomy*, 59, 5759
- Wang, B., Zhao, X., & Li, Z. 2014, *J. Cosmology Astropart. Phys.*, 11, 028
- Wang, X.-Y., & Liu, R.-Y. 2016, *Phys. Rev. D*, 93, 083005
- Waxman, E., & Bahcall, J. 1997, *Physical Review Letters*, 78, 2292
- Xiao, D., Mészáros, P., Murase, K., & Dai, Z.-G. 2016, arXiv:1608.08150

Table 1: Upper limit gamma-ray fluxes of the track-like neutrino events as observed by *Fermi*-LAT on the timescales of 12 hours and one year. The first column is the neutrino ID. The second column represents the energy of each neutrino event. The third and forth columns describe the positions of the neutrinos. The fifth column represents the median angular error  $R_{50}$ . The last two columns are the upper limit fluxes (0.2-100 GeV) over 12 hours and one year observations by *Fermi*-LAT around the neutrino detection time, respectively. The measured fluxes of the gamma-ray flare of PKS B1424-418 on the timescales of 12 hours and one year are also shown for comparison.

ID	Energy (TeV)	R.A. (°)	Dec. (°)	Angular error (°)	Flux( $\times 10^{-8}$ ) ph cm $^{-2}$ s $^{-1}$	Flux( $\times 10^{-10}$ ) ph cm $^{-2}$ s $^{-1}$
3	$78.7^{+10.8}_{-8.7}$	127.9	-31.2	1.4	8.05	3.75
5	$71.4^{+9.0}_{-9.0}$	110.6	-0.4	1.2	5.94	17.4
13	$253^{+26}_{-22}$	67.9	40.3	1.2	9.25	8.17
23	$82.2^{+8.6}_{-8.4}$	208.7	-13.2	1.9	9.80	19.9
38	$200.5^{+16.4}_{-16.4}$	93.34	13.98	1.2	18.1	35.0
44	$84.6^{+7.4}_{-7.9}$	336.71	0.04	1.2	32.4	4.19
45	$429.9^{+57.4}_{-49.1}$	218.96	-86.25	1.2	5.71	14.5
47	$74.3^{+8.3}_{-7.2}$	209.36	67.38	1.2	3.81	7.40
55 <sup>a</sup>	$2600 \pm 300$	110.34	11.48	0.27	11.3	8.61
160427A <sup>c</sup>	..	240.57	9.34	0.6 <sup>b</sup>	9.95	20.8
160731A <sup>c</sup>	..	215.109	-0.4581	0.35 <sup>b</sup>	12.5	24.7
160806A <sup>c</sup>	..	122.81	-0.8061	0.5 <sup>b</sup>	3.22	5.15
PKS B1424-418					$35.4 \pm 9.92$	$5889 \pm 60$

**Notes.**

<sup>a</sup> Neutrino event number 55 is a PeV event with  $R_{50} \approx 0.27^\circ$  (Schoenen & Raedel 2015).

<sup>b</sup> 160427A–Blaufuss (2016); 160731A–[http://gcnc.gsfc.nasa.gov/notices\\_amon/6888376\\_128290.amon](http://gcnc.gsfc.nasa.gov/notices_amon/6888376_128290.amon); 160806A–Cowen (2016).

<sup>c</sup> For the neutrino events with number 160427A, 160731A, and 160806A, their deposited energy are not given in the literatures or GCN Circulars.

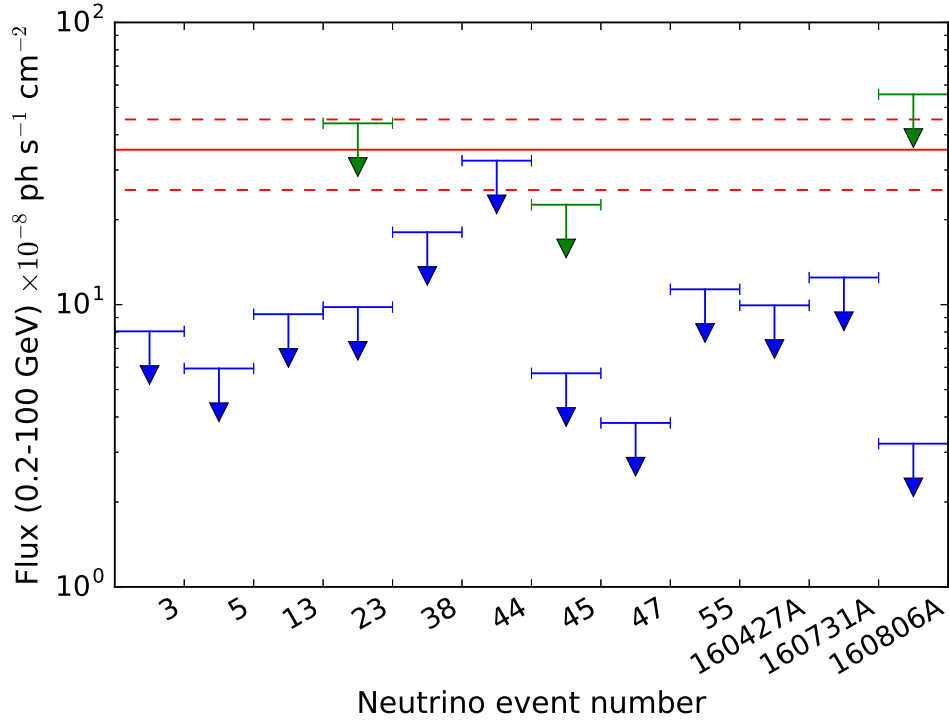


Fig. 1.— Comparison of the upper limit gamma-ray fluxes on the timescales of 12 hours and  $\sim 1000$  s, as reported in Table 1 (blue data) and Table 3 (green data) respectively, with the flux of the gamma-ray flare (red lines) from PKS B1424-418. The dashed red lines indicate the one  $\sigma$  flux range of the gamma-ray flare from PKS B1424-418.

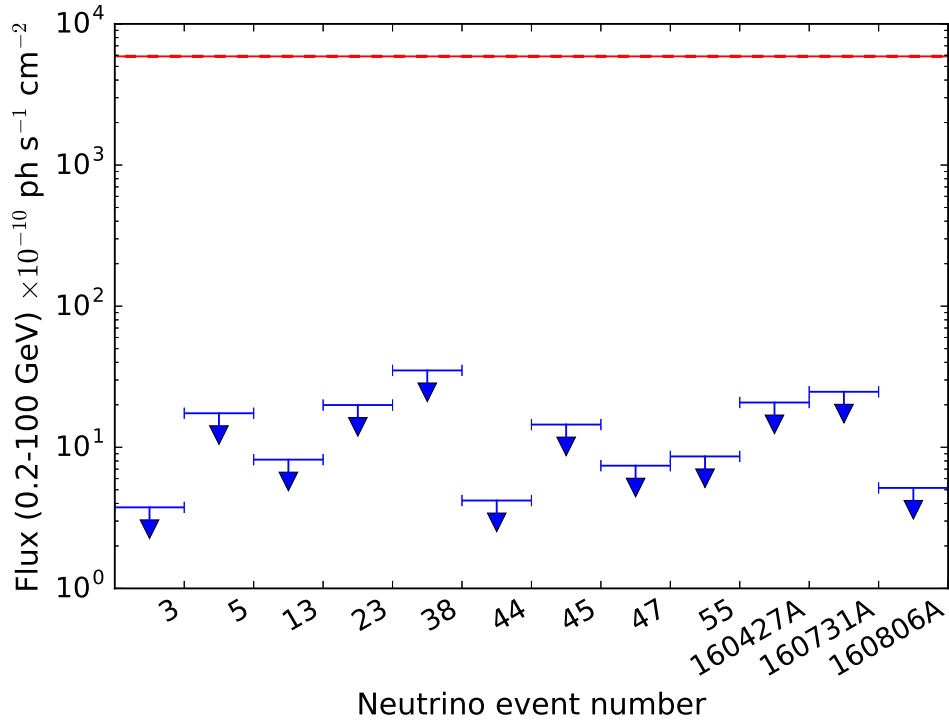


Fig. 2.— Upper limit gamma-ray fluxes of the track-like neutrino events for one year *Fermi*-LAT observations, as reported in Table 1. The flux of the gamma-ray flare of PKS B1424-418 (red lines) is presented for comparison.

Table 2: 3FGL sources that are found around the positions of the IceCube track-like neutrino events. The energy fluxes (in unit of  $10^{-11}$  erg cm $^{-2}$  s $^{-1}$ ) for one year *Fermi*-LAT observations are presented for sources only with  $TS > 25$  (under each 3FGL source name respectively).

ID	$R_{50}$	$2R_{50}$			
3		J0825.8-3217			
5	J0725.8-0054 $1.09 \pm 0.19$	J0721.5-0221			
13		J0423.8+4150 $2.82 \pm 0.31$			
23		J1349.6-1133 $4.61 \pm 0.23$	J1351.8-1524	J1355.0-1044	J1400.5-1437 $0.77 \pm 0.17$
44	J2227.8+0040 $0.62 \pm 0.16$	J2223.3+0103			
47		J1404.8+6554 $0.32 \pm 0.09$			



Table 3: Upper limit gamma-ray fluxes of the three IceCube track-like neutrino events that locate within the *Fermi*-LAT’s field of view at the neutrinos detection time. The first column is the neutrino ID, the second column is the time interval when the angular distance between the neutrino position and the *Fermi*-LAT boresight is less than  $70^\circ$ , and the last column is the upper limit flux in 0.2-100 GeV.

ID	Time+ $T_0$ (s)	Flux $10^{-7} \text{ ph cm}^{-2} \text{ s}^{-1}$
23	[-660,950]	4.39
45	[-1070,1910]	2.26
160806A	[-2080,440]	5.56

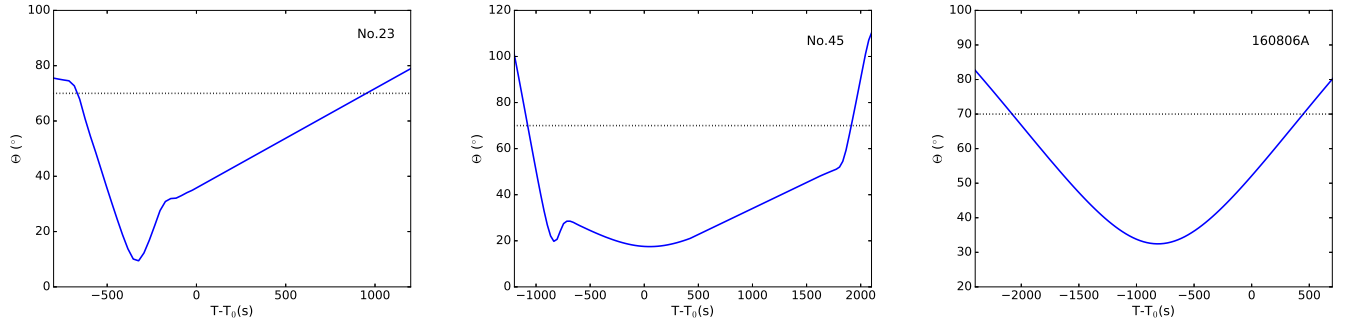


Fig. 3.— The angular distance ( $\Theta$ ) between the neutrino position and *Fermi*-LAT boresight as a function of time for the three IceCube track-like neutrino events.  $T_0$  is the neutrino detection time. The black horizontal dotted line represents  $\Theta = 70^\circ$ .

Table 4: *Swift*/BAT transient sources around  $2R_{50}$  of the IceCube track-like neutrino events. The last column is the angular separation between the positions of the neutrino and the X-ray sources. ‘LMXB’ means low-mass X-ray binary.

ID	Angular error( $^{\circ}$ )	X-ray sources	type	separation( $^{\circ}$ )
23	1.9	PKS 1352-104	Blazar	2.52
		Swift J1117.1-0933	LMXB	3.71
44	1.2	3C 445	Seyfert Galaxy	2.27
47	1.2	Mrk 279	Seyfert Galaxy	1.98

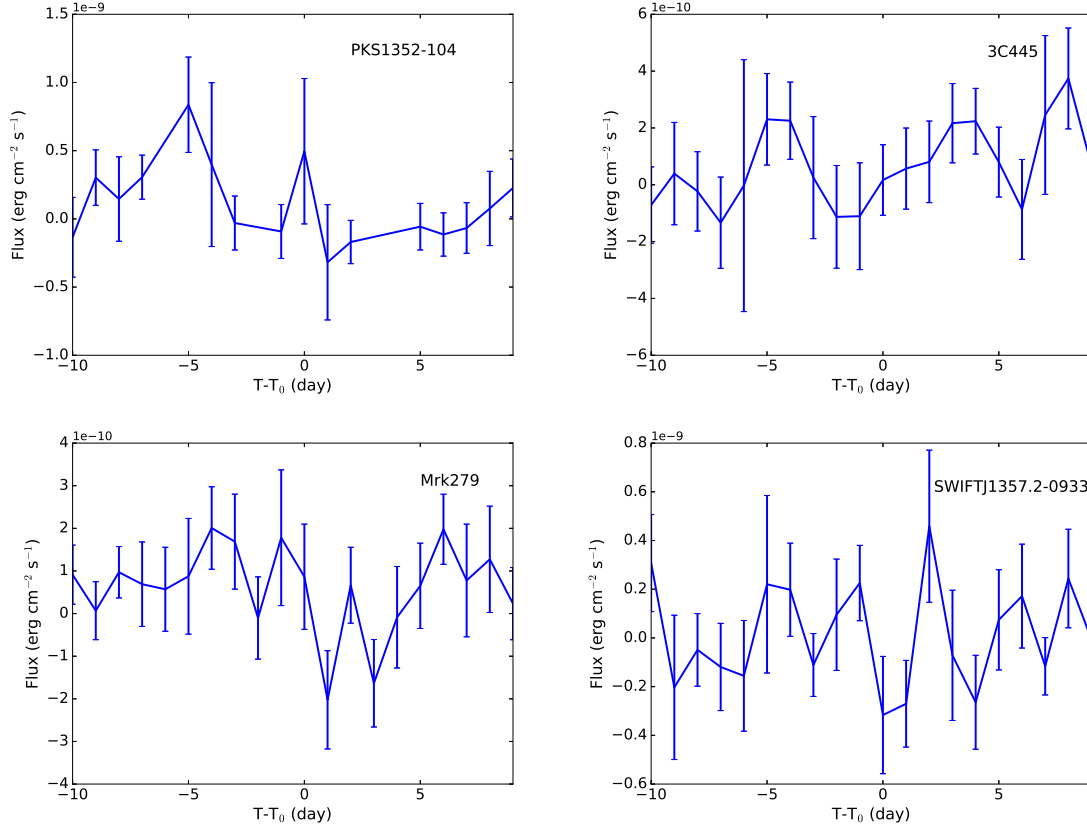


Fig. 4.— The hard X-ray light curves of *Swift*/BAT transient sources within  $2R_{50}$  of the neutrino positions. The neutrino detection time is denoted as  $T_0$ .